

## Self-assembling bilayers of palladiumthiolates in organic media

P JOHN THOMAS, A LAVANYA, V SABAREESH and G U KULKARNI\*  
Chemistry and Physics of Materials Unit, Jawaharlal Nehru Centre for  
Advanced Scientific Research, Jakkur PO, Bangalore 560 064, India  
e-mail: kulkarni@jncasr.ac.in

**Abstract.** Alkylthiolates of palladium forming a homologous series (butyl to octadecyl) have been prepared and characterized using X-ray diffraction and STM. The thiolates adopt an unusual bilayered lamellar structure, whose thickness is governed by the length of the alkyl chain. These mesophases melt in the temperature range, 60° to 100°C, with the melting point increasing linearly with the thiol chain length. There is evidence to suggest that the alkyl chains are orientationally disordered especially prior to melting.

**Keywords.** Self-assembling bilayers; palladiumthiolates; lamellar structures.

### 1. Introduction

Lipid bilayers have long been recognized as being central to molecular organization. Synthetic analogues mimicking biomembranes have been explored for potential applications in catalytic systems, solubilizing agents and drug delivery matrices. Following the pioneering efforts of Kunitake<sup>1</sup> and Fendler<sup>2</sup> it is known that many synthetic amphiphiles such as long chain fatty acids, quaternary ammonium salts with one, two or three chains or their sulfonium analogues all form bilayers under favorable conditions<sup>3</sup>. These bilayers have been characterized by employing a variety of techniques such as X-ray scattering, electron microscopy, circular dichroism, differential scanning calorimetry, Raman spectroscopy, NMR, UV-visible and infrared spectroscopy<sup>1-4</sup>. In the last few years, synthetic bilayers have been exploited to fabricate low dimensional biphasic lamellar structures or porous solids by mesoscale self-assembly<sup>5</sup>. Typical examples of such solids are nanocomposites of metal chalcogenides and oxides<sup>6</sup>.

A bilayer is normally constituted of a long chain amphiphile, with a hydrophilic head and a hydrophobic tail. The transfer of hydrocarbon chains into aqueous medium would accompany a free energy loss originating mainly from entropy<sup>3,7</sup> which drives the organic layer into ordered bilayers. Indeed, many synthetic bilayers have been realized in this manner<sup>1-4</sup>. In this context, self-assembly of amphiphiles in nonpolar organic media assumes significance<sup>8</sup> since such organization is considered to be driven by enthalpy rather than entropy<sup>9</sup>. Experimental successes in this pursuit have been few. Bilayers formed by per-fluoroalkyl derivatives in organic solvents<sup>8,9</sup> and by halo-bridged Pt composites in chloroform linked to long chain phosphates<sup>10</sup> are the only examples known to us.

In this paper, we report a study based on powder X-ray diffraction and scanning tunnelling microscopy of a series of palladium alkylthiolates, butyl to octadecyl, obtained

---

\*For correspondence

from toluene. Complexation of palladium ions with short alkane thiols has been known since the early work of Mann *et al*<sup>11</sup> who were intrigued by the waxy nature of the higher members and their high degree of association. Our work has shown that the palladium thiolates adopt an unusual lamellar structure, which is stable in organic liquid media. The free solubility in organic solvents distinguishes the Pd-thiolates from other heavy metal thiolates such as Ag and Cu, which precipitate out on forming a layered structure<sup>12,13</sup>. We have also investigated the melting behaviour of the alkyl chains in the thiolates and found some evidence for the presence of fluid rotator phases.

## 2. Experimental

The procedure adopted by us for the synthesis of palladium thiolates is as follows. To 5.0 mmol of Pd(OAc)<sub>2</sub> in toluene was added 5.0 mmol of the alkanethiol (butyl to octadecyl) and the resulting mixture was stirred vigorously. Following the reaction, the solution became viscous and the yellow colour deepened to orange yellow. Complete replacement of the acetate ligands by the thiolates was confirmed by estimating the acetic acid liberated. The obtained thiolates were freely soluble in organic solvents and such as toluene, methanol and heptane. A film obtained by drying a few drops of the toluene dispersion on a glass slide was used for X-ray diffraction (XRD) measurements. XRD patterns were obtained using Siemens Seifart 3000TT diffractometer employing CuK $\alpha$  radiation. A custom designed heating cell equipped with a precession thermometer was used for changing the temperature of the sample plate *in-situ* during X-ray diffraction measurements. Scanning tunnelling microscopy (STM) was performed on a Omicron Vakumphysic instrument equipped with a piezo with a sensitivity of 10 nm/V in all *x*, *y*, *z* directions. Samples for imaging were prepared by depositing a droplet of the dilute thiolate dispersion on freshly cleaved highly oriented pyrolytic graphite (HOPG) surface. Imaging was carried out in the forward I channel, typically with a bias voltage of 0.15 V, feedback current of 2 nA and a scan speed of 1000 nm/S.

## 3. Results and discussion

The XRD patterns obtained from nanocomposites of Pd and alkanethiols are shown in figure 1. All except the butanethiol complex are crystalline exhibiting patterns typical of a lamellar mesophase. The *d* spacings of the Bragg peaks vary as 1:2:3:4 and so on. For example, the pattern obtained from dodecylthiolate exhibits peaks with *d* values of 3.411, 1.711, 1.104, 0.876, 0.684 nm corresponding to the 001 to 005 reflections respectively. The (001) reflection, which is a direct measure of the bilayer thickness, increases from 2.298 nm in case of hexylthiolate to 4.778 nm in case of octadecylthiolate. The increase is linear with the number of methylene groups in the alkyl chain as can be seen from the inset of figure 1. A linear fit for this variation yields a slope of 0.248 nm per methylene and an intercept of 0.562 nm. It is instructive to examine these values closely to arrive at the structure of the diffracting lamellar solid. The C–C distance along the backbone plane of a fully extended all-trans conformer of an alkane chain is 0.123 nm. Thus, if the chains were to adopt the all trans form, a 0.247 nm increase in the thickness of the bilayer for every additional methylene group is to be expected<sup>14,15</sup>. This is indeed in close agreement with the experimentally obtained value of 0.248 nm per methylene unit. The structure of the head group could be ascertained from the intercept. We first carried out a search in Cambridge structural database<sup>16</sup> for unstrained sulphur

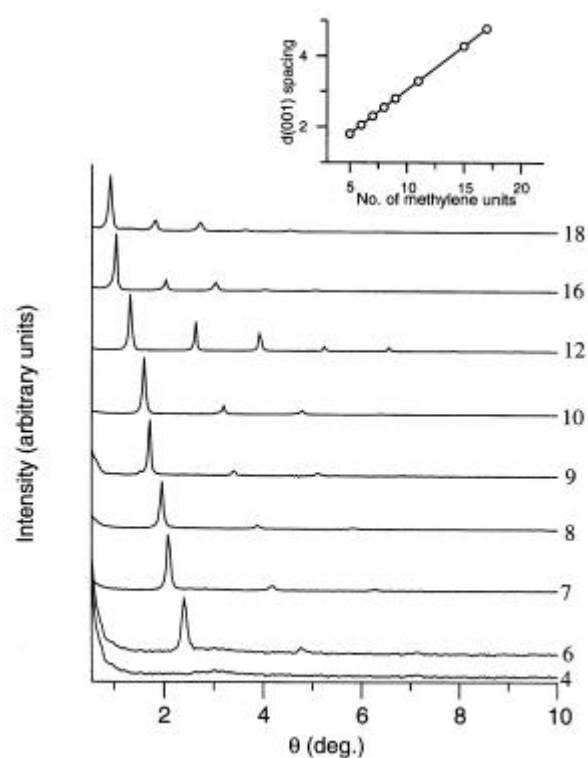


**Figure 1.** X-ray patterns obtained from nanocomposites of palladium with alkane thiols of different chain lengths (butyl to octadecyl). The numbers given alongside show the number of C atoms in the parent thiol. Inset shows the variation of the observed  $d_{001}$  peak position with the number of methylene groups in the alkane chains.

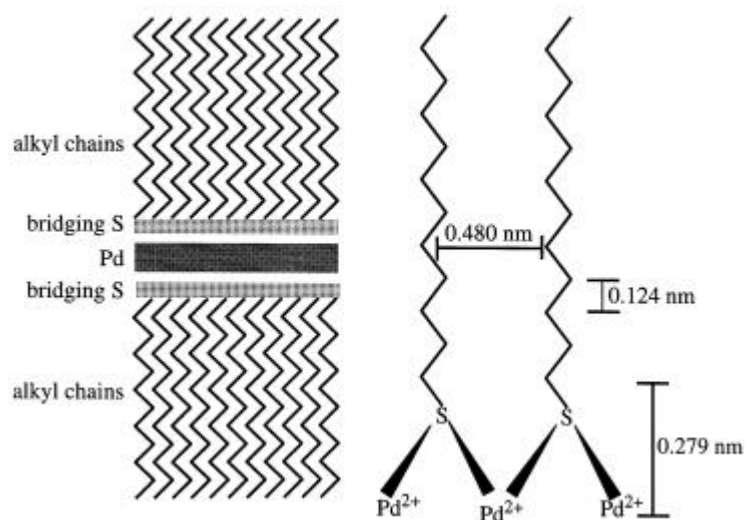


**Figure 2.** A schematic illustration of the structure of palladiumdecylthiolate.

bridged Pd motifs containing C–S bonds. The mean values obtained from 15 hits are  $0.181 \pm 0.004$  and  $0.232 \pm 0.003$  nm for C–S and Pd–S bonds respectively. Therefore, the length of the C–S–Pd motif along the C–S bond is 0.279 nm. Since the diffraction is from a bilayer, twice this value (0.557 nm) should correspond to the intercept, which is indeed the case (0.562 nm). A schematic illustration of the structure of the nanocomposite is given in figure 2. Moreover, the sulphur bridged palladium configuration as shown is similar to that observed in single crystals of palladium *n*-propylthiolate<sup>17</sup> (see figure 3a). The crystal structure of Pd ethylthiolate obtained by us<sup>18</sup> is given in figure 3b. Thus, shorter thioliates can be crystallised out into hexameric ring structures in clear contrast to lamellar phases formed by the higher members.

We sought to image the lamellar mesophases formed by palladium thioliates using STM. Imaging was performed on a sample of dodecylthiolate obtained from toluene dispersion on a graphite substrate (figure 4). STM images reveal a large number of string-like features generally in bunches of four or five, with the lengths ranging between 30 and 65 nm (see figure 4a). The observed thickness of the strings,  $3.4 \pm 0.3$  nm closely matches the 3.29 nm  $d_{001}$  spacing.

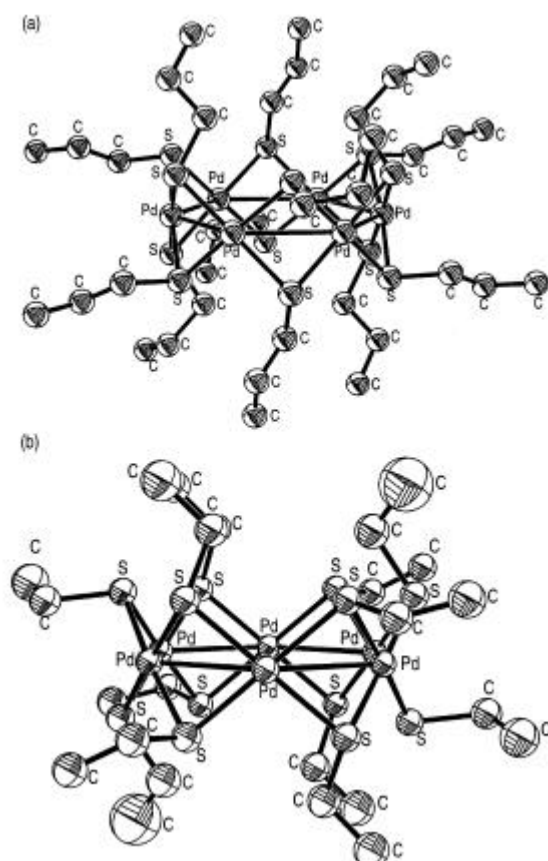


**Figure 3.** Hexameric Pd-ring motifs in the crystal structures of (a) Pd *n*-propylthiolate, (b) Pd ethylthiolate.

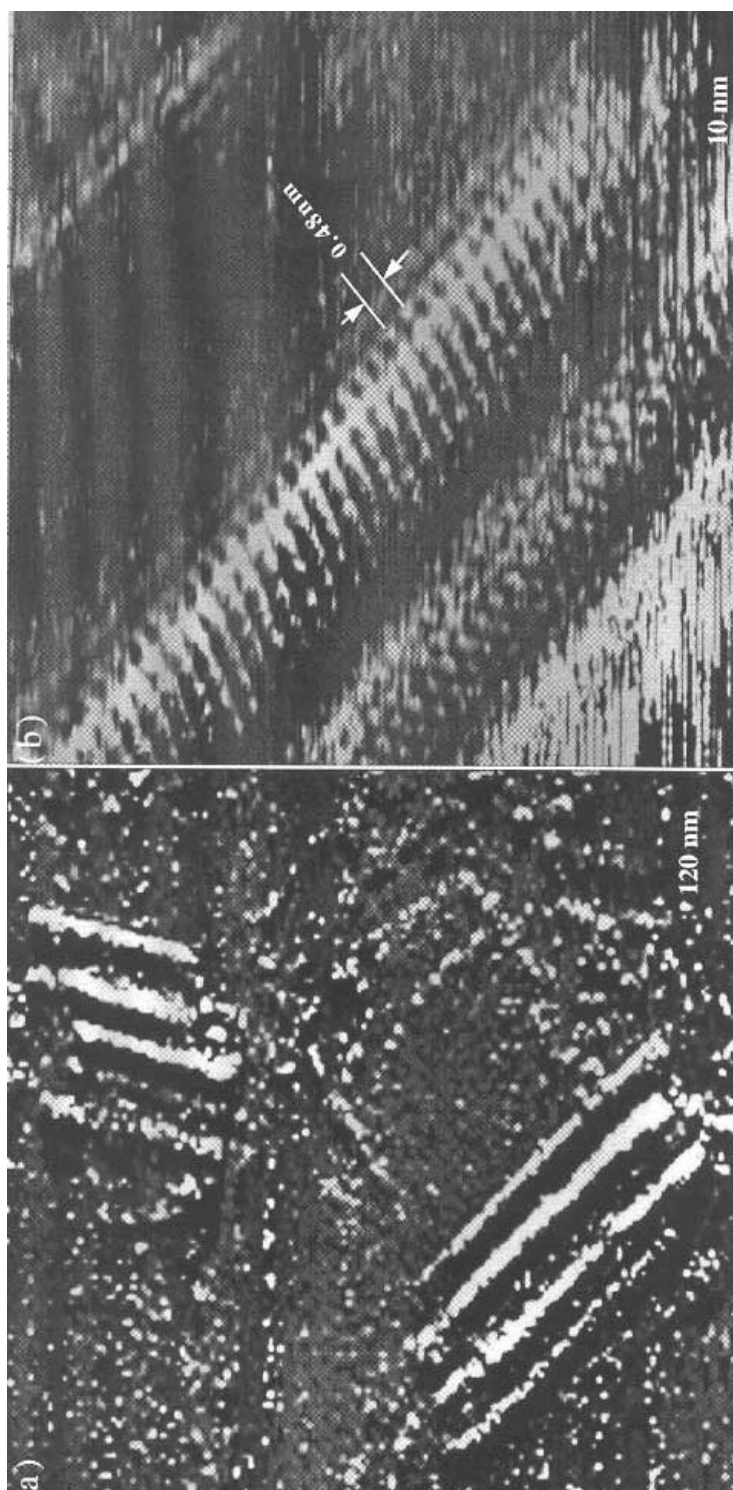


**Figure 4.** STM images showing the structure of the nanocomposite formed by palladium with dodecanethiol (500 mV, 2 nA).

Scanning in smaller areas reveals additional details (figure 4b). We observe hairy structures corresponding to alkyl chains with a uniform separation of 0.48 nm between them. Such a separation distance is also typical of self-assembled alkane thiol molecules on planar metal surfaces<sup>15</sup> and the other known metal thiolates<sup>12,13</sup>.

The supramolecular assemblies described above are readily obtained in a variety of solvents such as heptane, benzene, toluene, tetrahydrofuran, dichloromethane and acetic acid. The free solubility in all the above solvents, displaying a high degree of association<sup>11</sup> suggests that the thiolates adopt a bilayered structure in the organic medium, thereby joining the class of covalent amphiphiles. Similar lamellar phases are also obtained from water starting with an aqueous solution of  $\text{H}_2\text{PdCl}_4$  and a solution of alkanethiol in benzene. The versatility exhibited by these nanostructures is indeed remarkable.

In an effort to observe the lattice melting, the palladium thiolates were subjected to a controlled heat treatment in the *in-situ* XRD cell. The  $d_{001}$  peak was monitored in the heating and cooling cycles over the temperature range of 19° to 90°C. As a typical example, we show in figure 5, the  $d_{001}$  peak from decylthiolate for a few select temperatures. The 19° and 38°C peaks are slightly asymmetric and display shoulders at low angles. Above 40°C, the peak becomes narrower and symmetric. The peak position shifts by  $\sim 0.3^\circ$  before it vanishes above 70°C. On cooling, the peak intensity start regaining only below 50°C and the position shifts slightly towards lower angles. Interestingly, the peak is now symmetric and narrow close to room temperature unlike in a freshly formed lattice.

We obtained the diffractograms from the different thiolates at various temperatures. The variation in the intensity of the peak with temperature is shown in figure 6 for heptyl, decyl and dodecylthiolates as illustrative examples. We notice that in the case of heptylthiolate, the intensity decreases gradually in the range,  $\sim 42^\circ$  to 60°C. On the other hand, the peak intensities do not decrease monotonically in the case of decyl and dodecyl thiolates but instead exhibit two distinct regions interspersed by a plateau. The first region extends from 35° to 42°C in decylthiolate and from 40° to 57°C in dodecylthiolate. The corresponding ranges for the second region are 60° to 75°C and 72° to 85°C respectively. This variation of the diffraction peak seems to indicate the presence of two domains, which melt at different temperatures. The melting temperature was found to increase linearly with the thiol chain length as shown in the inset of figure 6. The slope of the line is 5.3°C per methylene unit. The behaviour on cooling is strikingly different in the three cases (figure 6). The heptyl thiolate stages no observable recovery, whereas the decyl and dodecyl lattices recover with intensities overshooting the room temperature values prior to melting by as much as 100%. We found that the hysteresis associated with crystallization of thiolates is critically dependent on the alkyl chain length. Thus, the  $d_{001}$  peak intensity recovered up to only 10% and 75% of the original in the case of octyl and nonyl thiolates.

A closer look at the  $d_{001}$  peaks in figure 5 help understand the stepwise decrease in intensity in case of the longer thiolates (decyl and dodecyl). We have fitted the peaks of the heating cycle with two Lorentzians by iteration, having given the initial peak positions at the shoulder and the main peak. The fits are also shown in figure 5. The intensity of the peak corresponding to the low angle shoulder fell sharply between 35° and 42°C (see Figure 7a). The intensity of the second peak, however, remained unchanged in this range. Its intensity decreases gradually at higher temperatures (figure 7a) accompanied by a small reduction in the  $d$  value of  $\sim 0.1$  nm (figure 7b). The two

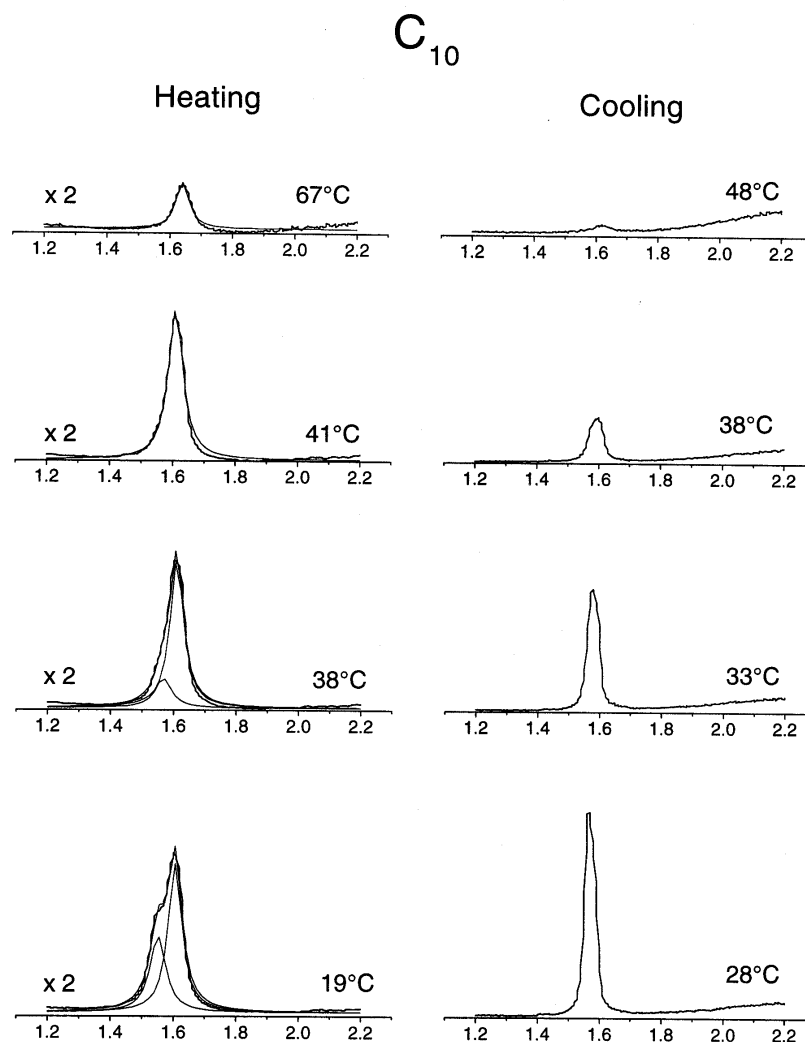


**Figure 5.** The  $d_{001}$  peaks at various temperatures during the heating and the cooling cycles. The asymmetric peaks at 19° and 38°C are corrected for nonlinear background and are fitted with two Lorentzian peaks.

steps in the variation of the total intensity (figure 6) therefore, correspond to successive vanishing of the two peaks. The peaks of the cooling cycle could be fitted satisfactorily with just one peak whose intensity increased monotonically with the  $d$  value decreasing by  $\sim 0.1$  nm (see figure 7b). The peaks from decyl thiolate separated from one another by 0.1 nm probably represent two different structural domains in the as-prepared nanocomposite arising from thiol chains adopting different rotator phases<sup>19</sup>. The existence of the thiol chains in fluid rotator phases would also account for the small changes in the  $d$  values. Indeed, long chain alkanes have been found to undergo a transition between as many as five different rotator phases before melting<sup>19</sup>. Upon cooling, the nanocomposite crystallizes to a single lamellar phase.

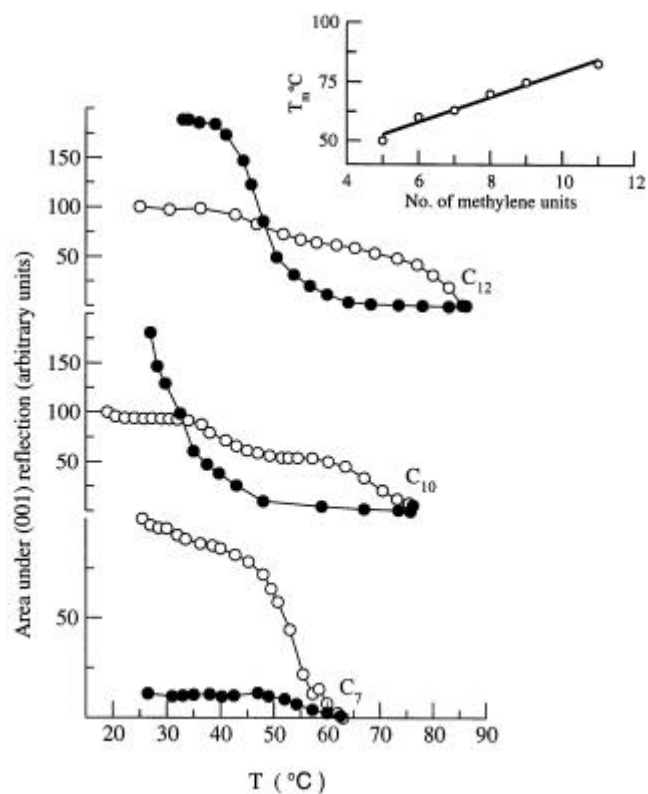


**Figure 6.** Variation in the intensity of the  $d_{001}$  peak with temperature in the case of heptane, decane and dodecanethiolates.

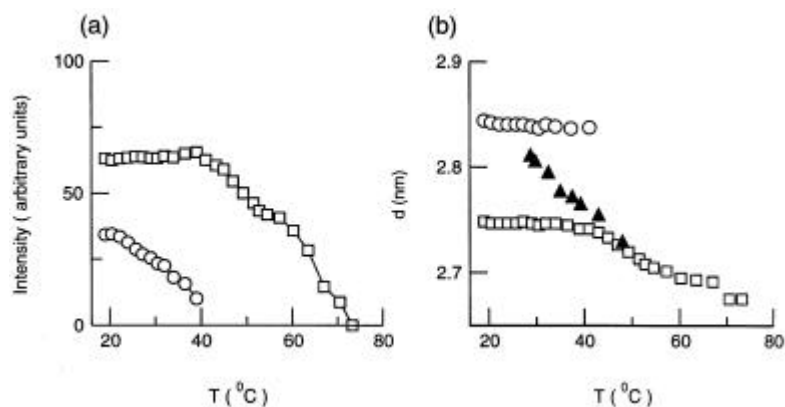


**Figure 7.** (a) Variation in the intensities of the fitted Lorentzian peaks in the case of decylthiolate with temperature; the peak under the shoulder, circles; the main peak, squares. (b) Variation in the  $d$  values of the fitted peaks. The variation corresponding to the cooling cycle is shown by filled triangles.

#### 4. Conclusions

Nanocomposites of palladium with alkane thiols of various lengths, hexyl to octadecyl, adopt robust lamellar structures, which can be obtained from a variety of solvents. The composites are bilayered with alkyl chains predominantly in the all trans conformation. Our study also provides evidence for an extended sulphur-bridged geometry of the head group. Shorter molecules such as butanethiol yield composites with no long range order, while ethane and *n*-propane thiols yield crystals containing hexameric Pd-rings. The lamellar phases formed by the higher members melt over a range of temperatures with the melting temperature increasing with the increasing chain length from 60° in hexylthiolate to 83°C in dodecylthiolate. The longer thiolates such as decylthiolate consist of two structural domains with different melting temperatures. The ability to recrystallize is also chain-length dependent, the longer ones recovering to well-annealed structures and the shorter thiolates remaining glassy. The observed hysteresis in lattice melting and the accompanying small changes in structure seem to indicate the presence of the chains in fluid rotator phases.

#### Acknowledgements

The authors thank Professor C N R Rao, FRS for useful discussion and encouragement. Thanks are also due to Ms T R Anupama for single crystal data collection.

#### References

1. Kunitake T 1992 *Angew. Chem., Intl. Ed. Engl.* **31** 709
2. Fendler J H 1980 *Acc. Chem. Res.* **13** 7
3. Furhop J H and Köning J 1994 *Membranes and molecular assemblies: The synkinetic approach* (London: Royal Chemical Society)
4. Okahata Y, Ando R and Kunitake T 1981 *Ber. Bunsenges. Phys. Chem.* **85** 789; Thompson D H, Wong K F, Humphry-Baker R, Wheeler J J, Kim J-M and Rananavare S B 1992 *J. Am. Chem. Soc.* **114** 9035; Kunitake T, Shimomura M, Kajiyama T, Harada A, Okuyama K and Takayanagi M 1984 *Thin Solid Films* **121** L89
5. Neeraj S and Rao C N R 1998 *J. Mater. Chem.* **8** 279
6. Bagshaw S A and Pinnavaia T J 1996 *Angew. Chem., Intl. Ed. Engl.* **35** 1102
7. Israelachvili J N 1992 *Intermolecular and surface forces* (London: Academic Press)
8. Ishikawa Y, Kuwahara H and Kunitake T 1989 *J. Am. Chem. Soc.* **111** 8530
9. Ishikawa Y, Kuwahara H and Kunitake T 1994 *J. Am. Chem. Soc.* **116** 5579
10. Kimizuka N, Oda N and Kunitake T 1998 *Chem. Lett.* 695
11. Mann F G and Purdie D 1934 *J. Chem. Soc.* 1549
12. Dance D, Fisher K J, Banda R M H and Scudder M I 1991 *Inorg. Chem.* **30** 183
13. Sandhyarani N and Pradeep T 2001 *J. Mater. Chem.* **11** 1294
14. Müller A 1930 *Proc. R. Soc.* **A127** 417
15. Dubois L H and Nuzzo R G 1992 *Annu. Rev. Phys. Chem.* **43** 437
16. Allan F H and Kennard O 1993 *Chem. Design Automata News* **8** 131
17. Kunchur N R 1968 *Acta Crystallogr.* **B24** 1623
18. Submitted to Cambridge Crystallographic Database, Ref. Code CCDC 167726
19. Müller A 1932 *Proc. R. Soc.* **A138** 514; King H E, Sirota E B, Shao H and Singer N M 1993 *J. Phys. D: Appl. Phys.* **B133** 26